Research Square

Preprints are preliminary reports that have not undergone peer review.
They should not be considered conclusive, used to inform clinical practice,
or referenced by the media as validated information.

Medieval Towers of Euboea: An Approach to construction phases with Radiocarbon Dating and Mortar Analysis

ADAMANTIA PANAGOPOULOU

a.panagopoulou@inn.demokritos.gr

National Centre of Scientific Research "Demokritos"

ANNO HEIN

National Centre of Scientific Research "Demokritos"

YIANNIS MANIATIS

National Centre of Scientific Research "Demokritos"

ANDREW BLACKLER

Hellenic Society for Near Eastern Studies (HSNES)

GEORGIOS POLYMERIS

National Centre of Scientific Research "Demokritos"

BENJAMIN CUTILLAS VICTORIA

Grupo de Investigación en Arqueología Prehistórica, Universidad Complutense de Madrid

IOANNIS ILIOPOULOS

Keramos Research Group

ALEXANDRA KOSTARELLI

Ephorate of Antiquities of Euboea (EAE)

JOANITA VROOM

Leiden University

Research Article

Keywords: Medieval Towers, Euboea, Radiocarbon dating, Chronology, Construction Phases, Mortar Technology

Posted Date: March 27th, 2026

DOI: https://doi.org/10.21203/rs.3.rs-9124055/v1

License: This work is licensed under a Creative Commons Attribution 4.0 International License.
Read Full License

Additional Declarations: No competing interests reported.

Medieval Towers of Euboea: An Approach to construction phases with Radiocarbon Dating and Mortar Analysis

A.P. Panagopoulou[(1)*], A. Hein[(1)], Y. Maniatis[(1)], A. Blackler[(2)], G.S. Polymeris[(1)], B. Cutillas Victoria[(1,3)], I. Iliopoulos[(4)], A. Kostarelli[(5)], J. Vroom[(6)]

(1) Laboratory of Archaeometry, Institute of Nanoscience and Nanotechnology, National Center for Scientific Research "Demokritos", 15341 Aghia Paraskevi, Attiki, Greece.
(2) Hellenic Society for Near Eastern Studies (HSNES), Chalkida, Greece.
(3) Grupo de Investigación en Arqueología Prehistórica, Universidad Complutense de Madrid.
(4) Keramos Research Group, Department of Geology, University of Patras, 26504 Rio, Greece.
(5) Ephorate of Antiquities of Euboea (EAE), Arethousa Museum, Hellenic Ministry of Culture, Chalkida, Greece.
(6) Faculty of Archaeology, Leiden University, Einsteinweg 2, 2333 CC Leiden, Netherlands.

***Corresponding author:** A. Panagopoulou: a.panagopoulou@inn.demokritos.com

ORCID numbers
0009-0002-6102-9408 (A. Panagopoulou)
0000-0002-5850-8144 (I. Iliopoulos)
0000-0002-9972-429X (G.S. Polymeris)
0000-0002-6358-4176 (B. Cutillas-Victoria)
0000-0001-8120-8978 (Y. Maniatis)
0000-0002-7793-0076 (J. Vroom)

Abstract

Central Greece once contained over 200 medieval towers, approximately two-thirds of which were located on Euboea. Many still dominate the landscape around Chalcis, either within village centers or on isolated hilltops. From the early medieval period onward, the region underwent successive political transitions, from Byzantine authority centered at Thebes to Latin, Catalan, Florentine, and Venetian control after 1204, culminating in the Ottoman conquest of Chalcis in 1470. Within this context of political instability between the late thirteenth and early fifteenth centuries, this pilot study investigates the chronology and construction phases of the Euboean towers. An integrated approach was applied, combining radiocarbon dating of wooden structural elements with the analytical characterization of mortars to assess their chronology and manufacturing technology. Radiocarbon dating indicates that all towers were constructed between 1270 and 1434 cal AD. More precise construction phases were established for three towers through wiggle-matching: Mistros (1283–1323 cal AD), North Mytikas (1330–1374 cal AD), and Skounteri (1391–1414 cal AD). Complementary analyses of mortars, including optical microscopy, portable X-ray fluorescence (pXRF), petrography, scanning electron microscopy with energy-dispersive spectroscopy (SEM–EDS), and X-ray diffraction (XRD), reveal compositional variability reflecting different preparation techniques and the selective use of local resources. Evidence for two construction phases was identified at Bailelekas and North Mytikas. The integration of high-resolution radiocarbon dating with mineralogical and geochemical analyses provides new insights into the multi-phased construction history of Euboean towers and demonstrates the value of an interdisciplinary approach for the study of medieval fortifications.

Keywords: Medieval Towers, Euboea, Radiocarbon dating, Chronology, Construction Phases, Mortar Technology

1. INTRODUCTION

Classified as Internal | Intern

1.1 A concise historical and geographical context

The region of Central Greece extends 150 kilometers north from the city of Athens to the foothills that separate it from the plains of Thessaly. It also includes Euboea (Εύβοια), an island that stretches 200 kilometers along its eastern shores and has been connected to the mainland by a short 30-meter bridge for over 2.500 years (Fig. 1). During the medieval period, three major cities became influential in this region. From around 700 CE, Thebes served as the administrative center of the Byzantine prefecture (*thema*), known as *Hellas*. In the autumn of 1204, forces of the Fourth Crusade annexed Central Greece, and three Lombard lords from northern Italy started to rule Euboea with support from the Republic of Venice. They shared its capital, Chalcis (also known in medieval times as *Negroponte*), while the mainland was governed by the Burgundian De la Roche family established in Athens. After their disastrous defeat at the Battle of Halmyros (town of southern Thessaly) in 1311, a Catalan mercenary company took control of the mainland. The Catalans killed Walter De La Roche and almost all of his cavalry, and seized his Duchy of Athens (excepting only the Lordship of Argos and Nauplia). The Catalan Company nominated one of the surviving knights, Roger Deslaur, as their leader and new Duke of Athens by conquest. However, in 1388, the Catalans were replaced by the Acciaiuoli family from Florence. Furthermore, in 1390, the Venetian Republic absorbed Euboea into its expanding empire. In 1470, Ottoman forces under Sultan Mehmet II, having annexed the mainland, captured the fortress of Chalcis after a three-month siege, making it the capital of the region. From then on, it was known as the *Sançak of Egriboz* until Greece gained its independence in 1830.

Central Greece once hosted over two hundred medieval towers of various designs, with over a hundred located on Euboea Island alone. When traveling through the countryside surrounding the city of Chalcis, one of the most striking features of the landscape is the tall stone towers visible throughout the area. Many of these still stand today, often found in village centers or perched on remote hilltops (Blackler 2022; Vroom and Kane 2025). Their purpose, however, remains unclear: Who built them? When were they built? And why? These questions are some among the cornerstones of the research conducted by the 'Hinterlands of Medieval Chalcis Project' (HMC Project). The project's overall goal is to gain a better understanding of the relationship between the countryside and the city of Chalcis during the Byzantine, Latin, and Ottoman periods (between ca. mid-4th and mid-19th centuries CE). From 2021 onwards, the HMC Project, directed by Professor Dr. Joanita Vroom (Faculty of Archaeology, Leiden University) and Dr. Alexandra Kostarelli (Ephorate of Antiquities of Euboea), conducted various fieldwork seasons on the island of Euboea with permission of the Hellenic Ministry of Culture (Vroom et al. 2021, 2023; Vroom et al. forthcoming a-b; Vroom and Kane 2025). One aspect of this project was the sampling of mortar from a selection of towers in the region and the analysis of their elemental and mineralogical composition by a team led by Dr Andrew Blackler (historical topographer) funded by the UK-based Castle Studies Trust.

The research area of the HMC Project spans a series of sites totaling 29.942 square meters within the valleys defined by the Lelas and Messapion rivers, located to the north and east of the towns of Chalcis and Psachna in central Euboea. In this region, the remains of seventeen medieval freestanding towers have been recorded whilst many others have been documented in historical cartographic sources. They are usually rectangular constructions in shape (about 8 x 8 meters) with a wall thickness of 1.20 – 1.80 meters. Some survive to their full height (with a maximum height of between13 to 18 meters) and may have three or four floors. In addition, most Euboean towers have an entrance on the second floor (for safeguarding reasons) and many still have their crenellation (bifurcated) intact.

These towers were first reported and discussed in two articles by the British historian Peter Lock (1986; 1996) based on the work by a local Greek researcher Theodoros Skouras (1975; 2003), while their relative dating and role was analysed in another article by the same author (1989). From an architectural point of view, tower construction is based on rough-cut stone bonded with mortar and tile slips. It has remained similar for nearly a millennium, from the Byzantine through the Latin into the Ottoman period.

Classified as Internal | Intern

The relative dating of these towers using diagnostic pottery has been attempted, but was hindered until recently by the lack of accurate ceramic chronologies and typologies (although this has now changed with Vroom 2003, 2014, 2022). Lock (1989, p.137), while noting that those on the mainland and most on Euboea fit a feudal agricultural rather than strategic context, was forced to admit that *'it is impossible to fix the date of the towers of post-Byzantine Greece definitely'*.

M.K. Langdon, in a gazetteer of those around the city of Athens, simply refers to '*mortared towers'*, refraining from any attempt to date them (Langdon 1995, p. 475-476). Blackler argues that towers served multiple functions. Whilst most had a mixed agrarian, administrative, and safeguarding role, many played a strategic role in long-distance communication (Blackler 2020). In a later article (Blackler 2022), he tentatively identified potential safeguarding chains of towers and beacons connecting Thebes and Chalcis, apparently creating a safeguarding network extending down to Naxos in the central Aegean, possibly predating the Latin arrival in 1204. However, his analysis did not offer definitive dating for these towers. Other views see these medieval structures not so much as free-standing watchtowers, but as storage spaces for local products and residences of the elite (e.g., Loizou 2017; Vroom et al. forthcoming c).

Recognizing the dating hiatus in our knowledge of one of the most ubiquitous groups of medieval monuments on Euboea, not only within the research area of the HMC Project but also all over Greece, we applied a range of scientific techniques to determine date and identify possible phases of construction. This study focuses on the Euboean towers and aims to establish their chronology, as well as to identify and distinguish the different construction (and possible renovation) phases.

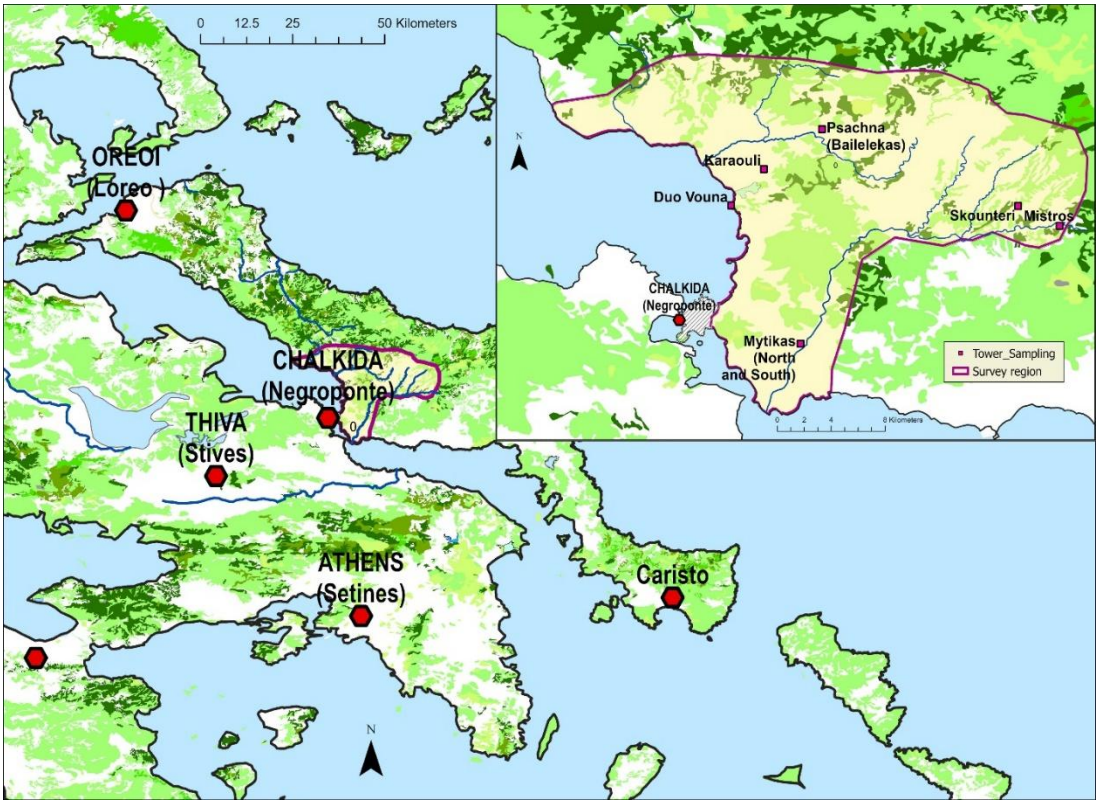


Fig. 1 Map of Central Greece with Survey area and Towers sampled; inset presents the sampling locations in more detail.

1.2 Resource aims

Towards this direction, the present study was undertaken to develop an integrated methodological framework for investigating the medieval towers of Euboea combining radiocarbon dating of wooden

Classified as Internal | Intern

beams and the analytical investigation of possible construction phases focusing on the mortars. Until now, the dating of towers in general, and those of Euboea in particular, has not been based on direct dating techniques, but primarily on comparative analysis of their morphological characteristics, as well as on, pottery and other finds, that may have emerged from rescue excavations conducted at the sites, given the current absence of other types of evidence (epigraphic and archival) (Blackler 2020, 2022; Kostarelli 2024; Vroom and Kane 2025; Vroom et al. forthcoming; Kostarelli and Blackler forthcoming). In this context, the present undertaking, carried out within the framework of the specific research program, seeks to complement these indirect, 'traditional' approaches to dating.

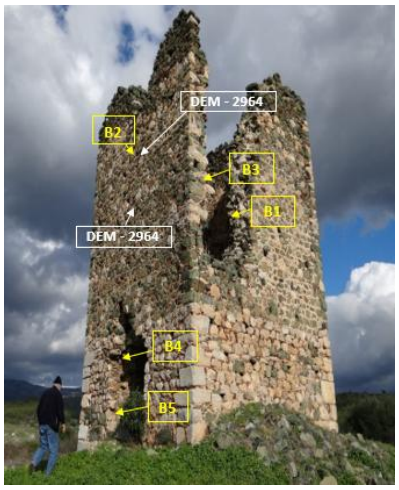
In the present study, an integrated methodological framework was adopted, incorporating the Radiocarbon dating as well as the investigation of microstructural characteristics alongside the analysis of the chemical and mineralogical composition of the tower materials. This approach is specifically designed to address the environmental context and architectural particularities of these monuments. The majority of the investigated towers are located in mountainous or otherwise uninhabited areas, often at considerable elevations and with substantial vertical development. Their exposed positions combined with more or less extreme environmental conditions, have rendered them particularly susceptible to advanced deterioration. The geographic setting of Euboea as an extended island surrounded by the sea, leads to a complex microclimatic regime characterized by strong winds, humidity fluctuations, and salt-laden atmospheres. These environmental conditions interact aggressively with structural materials, especially mortars and wooden beams, accelerating decay processes. In many cases, wooden beams have been entirely lost, while surviving fragments remain highly degraded. In view of this, the integrated study of mortars and surviving wooden beams proved essential for establishing chronology, reconstructing construction practices, and achieving a broader understanding of these structures.

1.3 Sampling procedure

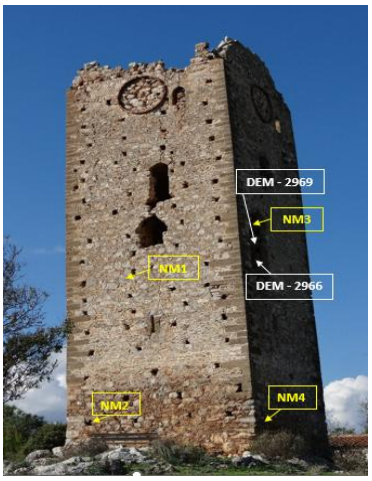
In general, all the medieval towers within the HMC project's research area were in an advanced stage of collapse. Seven different towers were chosen for sampling, from six different locations within the region. The photos from all towers are presented in Figure 2 while these locations are presented in the inset of Figure 3. Wood beam samples were collected for radiocarbon dating, as these were used to provide internal lateral structural integrity to their walls (Fig. 2). The criteria for selecting these towers included the quality and the size of each surviving beam; it was important that the beams were long and indicated prominent rings in their cross sections. We also ensured that the timber was not part of a subsequent repair or renovation, which would have been the case for beams used to support the multiple floors of the towers, but was part of the original construction phase.

At the same time, samples were also taken from various points of the mortar used to bind the rough stonework from which these had been constructed. Care was taken to avoid sampling areas affected by later external repointing or rendering of the walls, as such interventions could compromise the reliability of the analytical results. Furthermore, towers with different presumed roles and located in diverse settings were included in order to allow a broader interpretation of their potential functions. Wherever possible, samples (for both wood and mortar) were taken at different heights to understand whether construction had been undertaken within independent, subsequent phases. Mortar samples were selected based on visual observations outside of the towers in order to investigate whether the visual differences are due to different construction phases or due to corrosion. A total of 10 previously undated wood beam samples were collected from Bailelekas, North Mytikas, South Mytikas, Mistros, Skounteri and Karaouli, while for mortars, 17 samples were taken from Bailelekas, North Mytikas, South Mytikas, Karaouli and Dyo Vouna. Specifically, the towers of Bailelekas and North Mytikas were sampled at two distinct stratigraphic levels, corresponding to the lower and upper sections of the structure, in order to identify and differentiate earlier and later phases of construction. The samples were then sealed and dispatched to the NCSR «Demokritos» premises for processing and analysis.

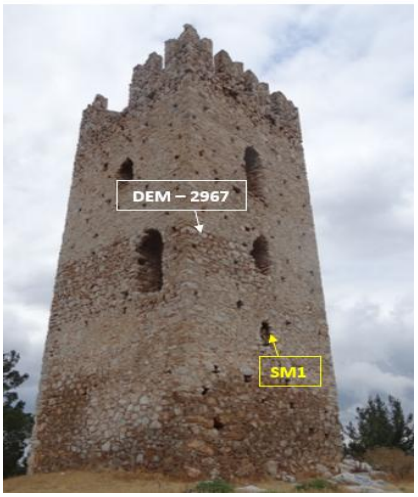
Classified as Internal | Intern



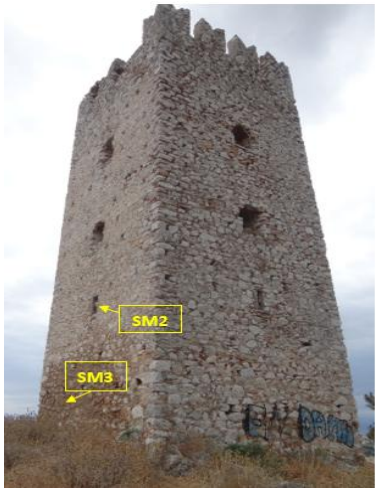
Bailelekas tower



North Mytikas tower



South Mytikas tower



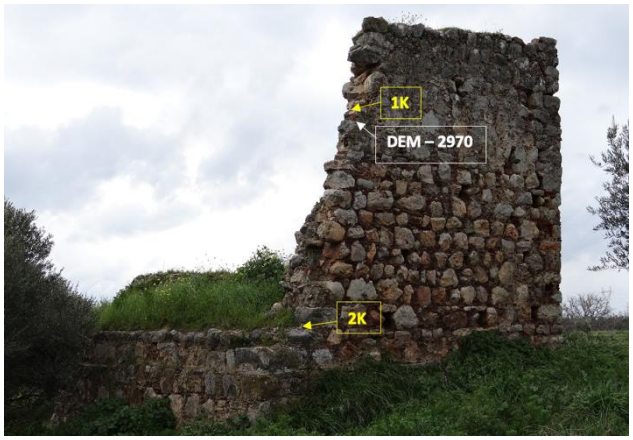


Mistros tower

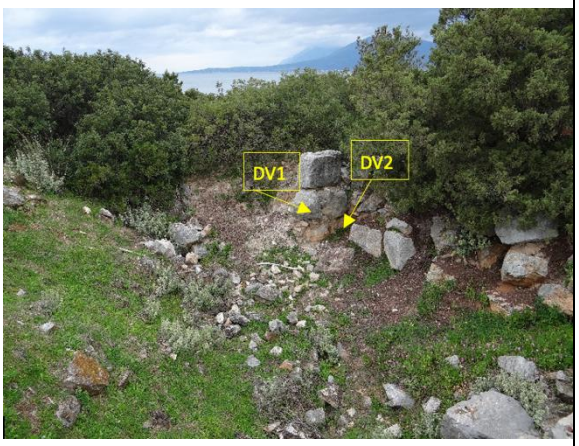


Skounteri tower

Classified as Internal | Intern



Karaouli tower



Dyo Vouna

Tower name	Location	Presumed role	GPS co-ordinates	Number of mortar samples	Number of wood samples
Bailelekas	By the river on the road leading from the upland plain to the coast	Estate centre, Control of movement along the road	38.58374, 23.68449	**5** (B1, B2, B3, B4, B5)	**2** (DEM-2964, DEM2965)
North Mytikas	Overlooking the river and irrigation channels	Headquarters of the river superintendent (*Potamarchis*)	38.44499, 23.67134	**4** (NM1, NM2, NM3, NM4)	**2** (DEM-2966, DEM-2969)
South mytikas	Overlooks river and agricultural land	Estate centre	38.44426, 23.67054	**3** (SM1, SM2, SM3)	**1** (DEM-2967)
Skounteri	Interior hilltop close to a strategic north-south road	Location of strategic military reserve	38.53407, 23.81535	-	**2** (DEM2963, DEM 2972)
Mistros	Communication link from Skounteri to mountain road and village	Signal / watchtower	38.52088, 23.84318	-	**2** (DEM-2973, DEM-2974)
Karaouli	In flood plain next to major road	Control of road (tax point?)	38.55777, 23.64567	**2** (K1, K2)	**1** (DEM-2970)
Dyo Vouna	Overlooks sea and links to fortress of Chalkis and Karaouli tower	Coastal watchtower	38.53439, 23.62388	**2** (DV1, DV2)	-

Fig. 2 Photos of the Towers; names, locations, presumed roles, GPS coordinates, along with the number and type of the samples collected from each of the studied towers.

2. MATERIALS AND METHODS

2.1 Wood beam samples for radiocarbon dating

The Radiocarbon dating of all the samples was performed at the Radiocarbon Unit of the Laboratory of Archaeometry, NCSR 'Demokritos' (International laboratory code: DEM). From each wooden beam's cross-section, 10-16 of the outermost preserved rings were separated and dated, counting from the center

Classified as Internal | Intern

of the tree. An exception was one sample (DEM-2969) from which 29 rings were separated and collected because of the very narrow thickness of the rings. Due to erosion and loss as well as sawing by the ancient builders of the tree logs to make them rectangular, the preserved outermost rings dated are not necessarily those immediately below the bark, which, if preserved and dated, would have given a date closer to the date of fell.

To overcome this problem, before removing any piece of wood for dating from a wooden beam cross-section, the approximate number of rings missing up to the bark was estimated, using the thickness and density of the rings in each beam, the curvature of the rings, and the radius and shape of the beam. This information was used to introduce a correction factor to the date obtained from the outermost preserved rings for calculating the actual date of fell of the tree and, hence, the closest date to the construction of each tower or tower phase. Examples of wood beam cross-sections along with technical details on the sampling procedure are presented in Fig. 3.

For two wooden beams, namely Skounteri-2 and North Mytikas-2, which had a large number of tree rings adequate for obtaining five and four, respectively, sequential segments/samples including about ten tree rings each, were radiocarbon dated individually, and the Wiggle Matching Method was applied. This analysis involves matching the radiocarbon dates of each segment as part of a sequence to the 'wiggles' of the calibration curve, given the fact that the age difference between the ^{14}C dates of the segments is known since they represent sequential rings of the same tree. The simplest approach is to use a classical Chi-squared fit of the ^{14}C data to the ^{14}C calibration curve. This gives the calendar date where the data fit best and allows determining with high accuracy the outermost ring's date closest to the date of fell of the tree (Bronk-Ramsey et al. 2001). For the procedure, samples consisting of about ten tree rings were removed in a sequence starting from the outermost rings and moving towards the centre of the tree log. Sampling details of the segments received are shown in Fig. 3. Each sample was treated and measured separately as described below.



Sample **DEM-2966**, *North Mytikas -1*. Dated rings: 9 outermost, above crack.



Sample **DEM-2967**, *South Mytikas -1*. Dated rings: 7 outermost, above pin.



Samples **DEM-2963**; **DEM-3016 - DEM-3019,** *Skounteri-2*. Example of five groups of tree-rings separated producing five consecutive dated samples for Wiggle Matching.

Fig. 3 Photos of the cross sections for a selection of wood beams.

2.1.1 Preparation and Chemical Pre-treatment of the wood samples

For each radiocarbon date, about 17 g of dry wood from about 10-16 rings of each wooden beam were used, except the North Mytikas-2 sample (Fig. 3) from which we took 29 rings as discussed above. The wood was ground down with a grinding mill to small particles of sizes a few mm in cross-section, and put in a beaker with de-ionized water and in an ultrasonic bath for 15 minutes to remove any soil deposits.

Classified as Internal | Intern

Following that, the sample was placed in a Soxhlet extractor and washed with pure organic solvents in a sequence of Methanol-Acetone-Methanol and finally hot water in order to remove pollutants such as oils/grease, pitch, shellac/varnish, etc. The treatment in the Soxhlet lasted for about 100 cycles for each solvent.

The sample was subsequently put into a 4% solution of NaOH at 80ºC stirred well, and left in the water bath overnight. It was then transferred to an acid solution of 4% HCl - again at 80 °C - where it stayed for more than an hour, being continuously stirred. The sample was then neutralized with hot (100 °C) deionised water. The entire cycle was repeated several times until the water over the sample became clear. When the pre-treatment was finished, the samples were dried in a dryer oven at 100°C.

2.1.2 Combustion and measurement

The dry wood samples were then combusted using the de Vries-type continuous combustion system (Vries and Barendsen 1953; Münnich 1957) and converted to gaseous CO_2, which then passed through columns of $KMnO_4$ to remove sulphur compounds and water vapour traps to remove H_2O molecules. The CO_2 was then precipitated to calcium carbonate in a $CaCl_2/NH_4$ solution to remove all other gasses (O_2, N_2 etc.). Consequently, the calcium carbonate sample was turned again into CO_2 by treatment with HCl acid. At the final purification step, the traces of possible impurities of the radioactive radon gas were removed by conducting the sample through a column of active charcoal kept at 0 °C (Kromer and Münnich 1992). In the final step, the mass of every sample was adjusted to a fixed amount (8.5 g) and then measured in the counters.

The Radiocarbon Unit of NCSR "Demokritos" (International code: DEM) uses the gas (CO_2) proportional counting technique (GPC). The measuring system consists of 8 copper cylindrical gas proportional counters, four with a capacity of 4 litres and four with 3 litres. The counters are surrounded by continuous flow (Ar+10%CH_4) guard counters, which monitor all incoming environmental radiation and separate it electronically from the actual sample counts by an anti-coincidence system (Schoch et al. 1980). The samples are alternated every few days between the different counters and measured repeatedly, increasing in this way the accuracy and reliability of the results (Maniatis et al. 2010, 2016). The Radiocarbon ages are corrected for $\delta^{13}C$ (Stuiver and Polach 1977) and calibrated to calendar ages with the IntCal20 calibration curve (Reimer et al., 2020), using the software OxCal v.4.4.4 (Bronk Ramsey 2021).

2.2 Mortar samples

An integrated analytical approach was applied for the study of mortar sin order to investigate elemental and mineralogical composition as well as fabric and microstructure. The analysis was expected to reveal information concerning raw material selection and construction phases. For the elemental analysis, both portable X-Ray Fluorescence Spectroscopy (pXRF) and Scanning Electron Microscopy (SEM-EDS) were applied on polished sections of the mortar samples. The samples were prepared by embedding mortar fragments in epoxy resin, followed by curing and progressive polishing to obtain smooth, flat surfaces suitable for microstructural and compositional analysis. While SEM-EDS provides an estimation of the major element composition, from Z=11 (Na) to Z=26 (Fe), XRF additionally provides concentrations of minor elements and selected trace elements. For the determination of the mineralogical composition, X-Ray Diffraction (XRD) analysis was applied to powdered samples. The microstructure and mineralogical composition were also investigated by preparing thin-sections and examining them under a polarizing petrographic microscope. Over recent years, extensive research has been conducted on mortars, a field that is rapidly evolving with continuously emerging findings (Lancaster 2021; Rani et al. 2021; Ergenç et al. 2021; Pineda et al. 2022; Cantisani et al. 2022; Aškrabić et al. 2023; Fort et al. 2023; Varas-Muriel et al. 2024; Fort et al. 2024; Chuo et al. 2024; Sium et al. 2025).

Classified as Internal | Intern

2.2.1 Portable X-ray Fluorescence (pXRF)

The concentrations of minor and trace elements of the mortar samples were further studied with energy dispersive X-ray fluorescence using a handheld NITON XL3t GOLDD+ portable system (pXRF). For the present study the preset 'Cu/Zn Mining' calibration method was used, which had already been successfully tested for analyses of aluminosilicates and carbonates (Hein 2021). The measurements were carried out in air. The total duration of each measurement was 120 seconds collecting data in four different spectral energy ranges using different filters and voltages. Concentrations of elements with atomic numbers > 13 (aluminum) are reliably, while the indicative magnesium content(Z=10) is considerably affected by the absorption of the fluorescence radiation in air. During the measurement, the system was placed in a stand looking upwards and the samples were placed on top. The measurement area had an estimated diameter of circa 6 millimeters, and a photograph of each area was recorded with the integrated camera. The elemental analysis with pXRF is a non-destructive and non-invasive method, which can be applied even in situ (Bezur et al. 2019). In the present case study, however, pXRF has been applied on the existing polished sections, which had been prepared for the SEM, as they provided flat sections of the mortar stratigraphy from the potentially weathered surface into the presumably intact body. Each sample was analyzed in three different areas in order to obtain average values of the concentration taking into account the inhomogeneity of the coarse mortar structure. Thus, finally, 54 individual measurements were collected of the present assemblage of clay sealings. The composition will be given as elemental concentrations in wt%. Out of a total of 34 elements that were detected and monitored, 16 elements could be used for a statistical evaluation (Mg, Al, Si, P, S, Cl, K, Ca, Ti, V, Cr, Mn, Fe, Ni, Sr and Ba) as the other elements were either below the limit of detection or they were disregarded due to their known geochemical mobility. For standardization, the element concentrations were log-ratio transformed with the Ba concentrations as a common divisor. The standardized compositions were evaluated with hierarchical clustering in order to determine compositional patterns indicating the use of specific raw materials and/or admixtures.

2.2.2 Scanning Electron Microscopy (SEM-EDS)

Scanning electron microscopy (SEM) analyses were conducted on seventeen polished sections of the mortar samples using a Quanta Inspect FEI D8334 instrument equipped with an energy-dispersive X-ray spectroscopy (EDS) system. The SEM was operated at an accelerating voltage of 25 kV, and EDS spectra were acquired with a live time exceeding 120 s over selected areas of approximately 1 × 1 mm. Elemental compositions were quantified and expressed as oxide weight percentages (Na_2O, MgO, Al_2O_3, SiO_2, K_2O, CaO, and Fe_2O_3), normalized to 100%. For each sample, an average of three to five measurements was obtained from carefully selected, representative regions of interest, deliberately avoiding heterogeneous or altered zones to ensure analytical reliability (Goldstein et al. 2018).

2.2.3 Optical Microscopy (OM)

Petrographic analysis was conducted on six thin sections, corresponding to one representative mortar sample from each tower, using a Leica DM2700P polarising microscope equipped with a Leica MC190HD digital camera. Observations were performed under plane- and cross-polarised light at magnifications ranging from 25× to 400×. Petrographic analysis was carried out in order to characterize the binder, aggregate assemblage, textural relationships, and microstructural features of the examined mortars, following established methodological approaches for historic mortars (e.g., Elsen 2006; Pecchioni et al. 2025). Microstructural characterization included assessment of binder and aggregate characteristics, textural parameters (binder-to-aggregate ratio, packing density, grain-size distribution), and porosity.

Classified as Internal | Intern

2.2.4 X-ray Diffraction (XRD)

Bulk samples of seventeen mortar fragments were analyzed with X-ray diffraction (XRD) to investigate their mineralogical composition (Ali et al. 2022). For this, about 1 g of each sample was powdered and homogenized. The sample powder was placed in a sample holder and compressed with a glass slide. The XRD analysis was performed in the Minerals and Rock Research Laboratory, Department of Geology, University of Patras, Greece, employing a Bruker D8 Advance diffractometer with nickel-filtered Copper-K-alpha (Cu-Ka) radiation operating at 40 kV/40 mA and equipped with a Bruker LynxEye fast detector (Xanthopoulou and Iliopoulos 2023). The qualitative mineralogical analysis was performed using the DIFFRACplus EVA software (Bruker-AXS, Madison, WI, USA) based on the International Centre for Diffraction Data (ICDD) Powder Diffraction File (2006 version).

3. RESULTS

3.1 Radiocarbon dating of the wooden beams

Table 2 presents the radiocarbon results of all dated samples from wooden beams using the outermost preserved rings. The calibrated ages in calendar years (calAD) are also given with an overall 2σ (95.4%) probability. The approximate number of missing rings to the bark, for every beam sample, is also given, estimated as described in Section 3.2, along with the corrected calendar ages estimated for the fell of the tree, based on this correction. As can be seen in Table 3, the calibrated ages exhibit a rather wide range, which does not allow a more precise determination of the corresponding date of the tower construction phases. This widening of the calibrated age ranges is due to a wiggle in the calibration curve at 1310-1390 calAD (Figure 4), due to the sun's fluctuating radiation, which modulates the production of ^{14}C in the Earth's atmosphere. This wiggle causes a widening of the overall calibrated age range (both the uncorrected and corrected for the missing rings) or its splitting into two sub-ranges with different probabilities (Table 2, Figure 4) within an overall 95.4% probability. As can be seen in Table 3, the overall estimated date of fell (and hence the date of use of the timbers in the construction) for all the wooden beam samples dated from ca. 1270 calAD, the earliest, to 1434 AD, the latest, with 95% confidence. This range defines the overall time span within which the towers under study were constructed.

In an attempt to overcome the problem of the wiggle in the calibration curve, which causes this aforementioned widening of the calibrated age ranges (Figure 4) and obtain more precise dates for the fell of the trees, the Wiggle Matching method was applied as described above. This requires receiving and dating with radiocarbon at least four or five sequential samples from each beam section (Figure 4). Unfortunately, only two beam sections had enough tree rings to provide a set of samples containing more than 10 rings each. These were: Skouteri-2 sample and North Mytikas-2 sample. The individual dates ^{14}C dates obtained for these samples, with the corresponding numbers of tree rings, are shown in Table 3.

Since the radiocarbon age obtained for each sample reflects the concentration of ^{14}C in the atmosphere in the period the specific rings were created, the radiocarbon dates in sequence should show a variation similar to the calibration curve. Thus, the sequence of dates is fixed at a particular section of the curve, and each sample is dated with high accuracy. Table 3 presents all new data related to the wiggle matching analysis for each sample. The fitting of the radiocarbon dates from the sequential tree ring samples was subject to statistical treatment using Bayesian Analysis (Ramsey, 2008). For this analysis, we used the program OxCal v.4.4.4 (Bronk Ramsey 2021). The gap between the dated samples was defined from the central ring of the range of rings received for a sample to the center of the range of rings of the next consecutive sample; the latter is presented in the third column of Table 3.

Classified as Internal | Intern

The results of the statistically modeled calibrated ages of the five samples from Skounteri-2 and four samples from North Mytikas-2 fitted on the calibration curve, as well as the probability distribution and the weighted mean ages of the outermost ring *Boundaries* are shown in Figure 5. The tabulated results of this wiggle matching analysis are shown in Table 4. They show the range and the weighted mean value of the calendar dates obtained for the outermost ring boundaries and represent the date of the felling of the tree to the best possible accuracy. These dates should be very close to the date of use of this beam in the construction of the particular building phase of this specific tower in Table 4**.** Dating results for the particular construction phases of Skounteri and North Mytikas, following a wiggle matching analysis.

Classified as Internal | Intern

Table 1 Radiocarbon dating results of the outermost preserved rings from wooden beams and estimations for the missing rings for determining the date of the fell of the trees**.**

Laboratory Code	Tower and wood beam no.	Tree rings dated (no of central ring)	Samples for Wiggle Matching	Age ^{14}C (BP)	$\delta^{13}C$ (‰)
DEM–2963	Skounteri–2	57–69 (63)	Sample–1 (Outermost rings)	596 ± 30	–24.35
DEM–3016	Skounteri–2	43–55 (49)	Sample–2	647± 30	–23.78
DEM–3017	Skounteri–2	30–42 (36)	Sample–3	671± 30	–23.91
DEM–3018	Skounteri–2	17–29 (23)	Sample–4	642 ± 30	–23.96
DEM–3019	Skounteri–2	1–16 (8.5)	Sample–5 (Innermost rings)	602 ± 30	–23.74
DEM–2969	North Mytikas–2	43–72 (57)	Sample–1 (Outermost rings)	622 ± 30	–24.93
DEM–3020	North Mytikas–2	28–42 (35)	Sample–2	666 ± 30	–25.44
DEM–3021	North Mytikas–2	13–27 (20)	Sample–3	700 ± 30	–25.10
DEM–3022	North Mytikas–2	1–12 (6.5)	Sample–4 (Innermost rings)	720 ± 30	–25.05

Classified as Internal | Intern

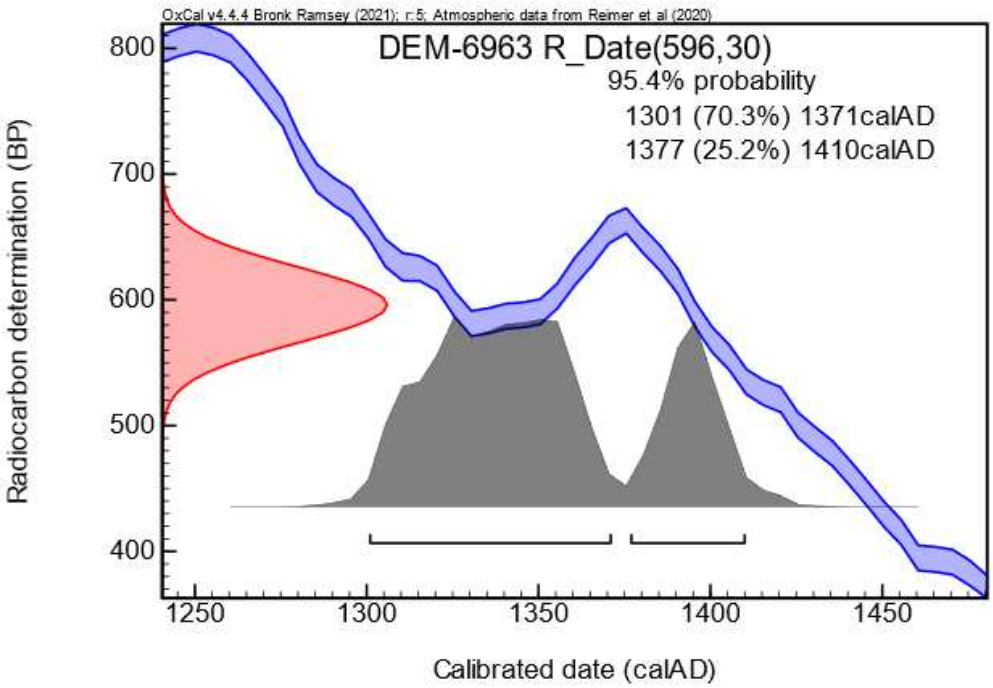


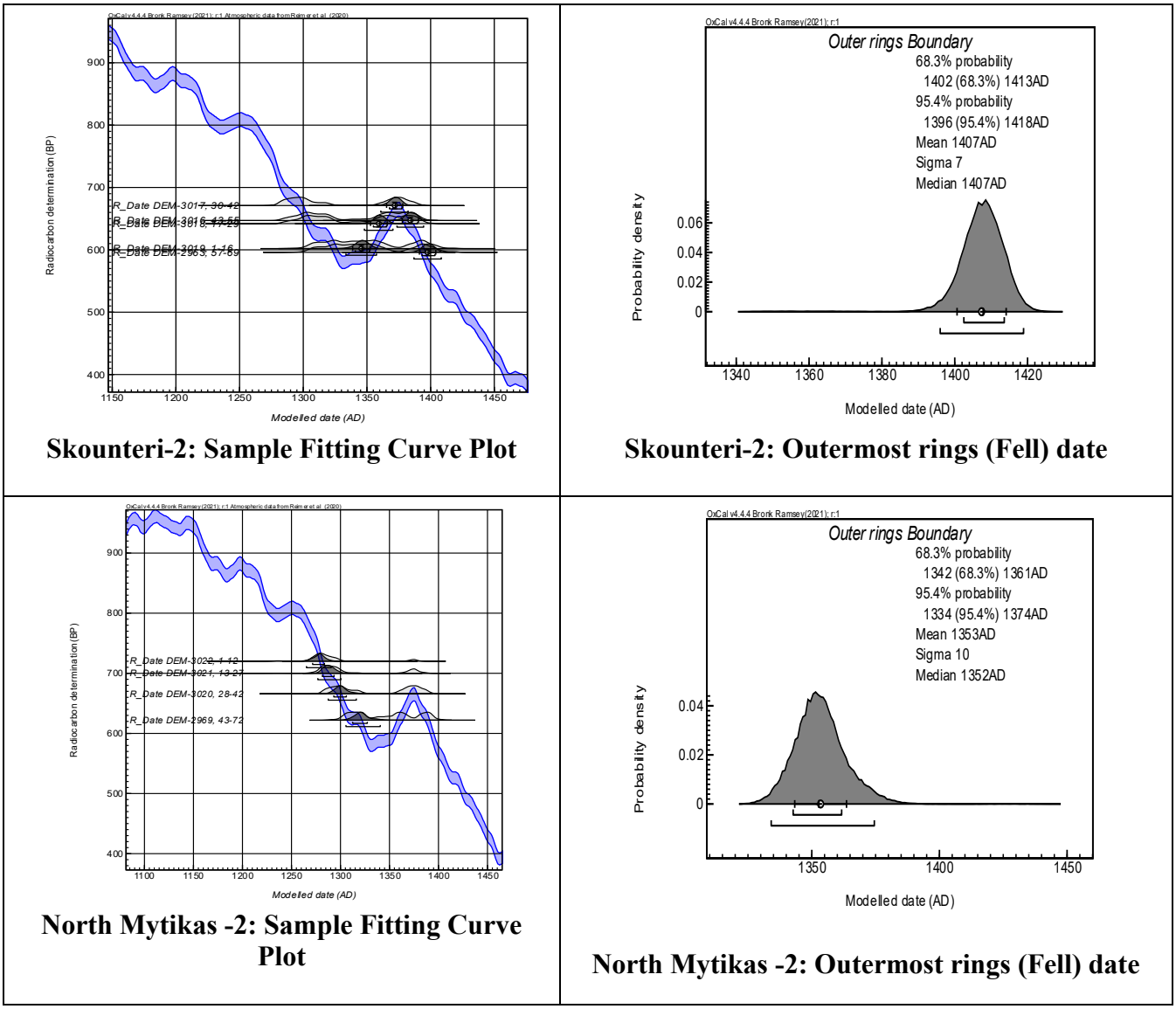
Fig. 4 An example of calibrated age, showing the wiggle in the calibration curve that causes widening of the calibrated ages and splitting of the ranges.

Classified as Internal | Intern

Table 2 The number of tree rings dated and the corresponding radiocarbon dates of the sequential samples from Skounteri-2 and North Mytikas-2 beam sections used for Wiggle matching analysis.

Laboratory Code	Tower and wood beam no.	Tree rings dated (no of central ring)	Samples for Wiggle Matching	Age ^{14}C (BP)	δ^{13}C (‰)
DEM – 2963	Skounteri-2	57 – 69 (63)	Sample-1 (Outermost rings)	596 ± 30	-24.35
DEM – 3016	Skounteri-2	43 – 55 (49)	Sample-2	647± 30	-23.78
DEM – 3017	Skounteri-2	30 – 42 (36)	Sample-3	671± 30	-23.91
DEM – 3018	Skounteri-2	17 – 29 (23)	Sample-4	642 ± 30	-23.96
DEM – 3019	Skounteri-2	1 – 16 (8.5)	Sample-5 (Innermost rings)	602 ± 30	-23.74
DEM – 2969	North Mytikas -2	43 – 72 (57)	Sample-1 (Outermost rings)	622 ± 30	-24.93
DEM – 3020	North Mytikas -2	28 – 42 (35)	Sample-2	666 ± 30	-25.44
DEM – 3021	North Mytikas -2	13 – 27 (20)	Sample-3	700 ± 30	-25.10
DEM – 3022	North Mytikas -2	1 – 12 (6.5)	Sample-4 (Innermost rings)	720 ± 30	-25.05

Classified as Internal | Intern



Skounteri-2: Sample Fitting Curve Plot

Skounteri-2: Outermost rings (Fell) date

North Mytikas -2: Sample Fitting Curve Plot

North Mytikas -2: Outermost rings (Fell) date

Fig. 5 Left-side plots show the wiggle matching calibration plots of the sequential samples for each wooden beam. The right-side plots show the final calibrated age of the outermost rings, corrected for the missing rings.

Classified as Internal | Intern

Table 3 Accurate radiocarbon dating results for the construction of towers (where possible), following a specific combination of statistical analysis.

Tower	Statistical Analysis	Date range (95.4%) (calAD)	Weighted Mean Date (calAD)
Mistros	Statistically Combined	1283–1323	**1303 ± 19**
North Mytikas	Wiggle Matching & Statistically Combined	1330–1374	**1352 ± 22**
Skounteri	Wiggle Matching & Statistically Combined	1391–1414	**1402 ± 11**

Sample/Tower	Construction phase	Date range (95.4%) (calAD)	Weighted Mean Date (calAD)
Skounteri–2	Lower	1396–1418	**1407 ± 7**
North Mytikas–2	Upper	1334–1374	**1353 ± 10**

Classified as Internal | Intern

3.2 **X-Ray Fluorencese Spectroscopy (pXRF)**

Non-invasive energy-dispersive X-ray fluorescence using pXRF was applied for an initial compositional characterization of the mortar samples in view of their compositional variation and the identification of distinct compositional patterns. Initially, pXRF analysis was conducted on all mortar fragments; subsequently, seventeen samples were selected for polishing and further analysis using both pXRF and SEM–EDS. Figure 6 presents a principal component analysis (PCA) of the normalized pXRF data indicating distinct mortars being used for the wall constructions at different sites. The remaining samples were allocated for additional laboratory analyses, including XRD and petrographic examination. For this, particular consideration was given to any chemical indication of potential deterioration patterns, such as peculiar salt content or increases in Sulphur's concentrations. The towers are commonly located on hills or elevated terrain and, thus, they are particularly exposed to the environment. Notable levels of deterioration of the mortar compounds can often be observed even by naked eye. The sampling strategy supported by pXRF was focused on selecting the least affected components preferably representing the original elemental composition.

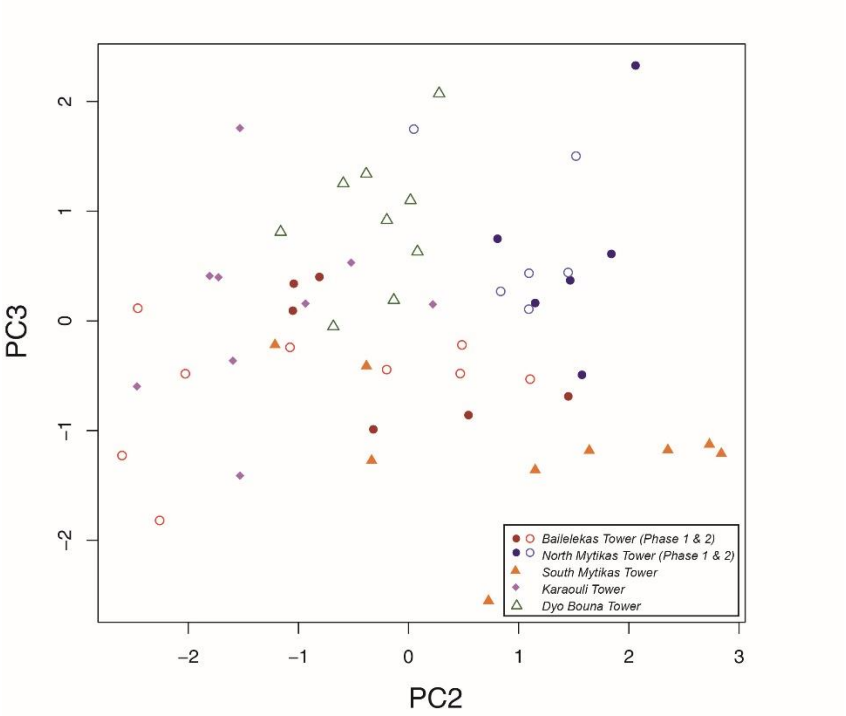


Fig. 6 Principal Components Analysis (PCA) of the normalized chemical compositions of mortar samples collected from the towers determined by pXRF: The symbols indicate the individual towers from which the mortar samples were collected. While PC2 is loaded mainly with Al and K, PC3 is loaded with Si.

3.3 Elemental Composition of Mortars (SEM-EDS Analysis)

SEM-EDS investigations show that the main oxide components are CaO, SiO_2, MgO, and $Al2O_3$, which are consistently present in all mortar samples examined. In contrast, Fe_2O_3, K_2O, and Na_2O are used as discriminant characteristics for compositional classification because their occurrence and relative abundances are more variable and appear to be closely related to mortar type. The prevalence of calcium and magnesium in the binder matrix, which reflects the extensive usage of calcareous and, for the most part, magnesian raw materials, is a notable feature shared

Classified as Internal | Intern

by most of the samples. A notable exception is observed in the mortar from the upper level of the Bailelekas tower, where magnesium is entirely absent from the matrix. As further shown in Fig. 6, both SEM–EDS and portable X-ray fluorescence (pXRF) analyses consistently confirm this compositional peculiarity, supporting the validity of the analytical results and highlighting the technological or provenance-related significance of this deviation (Fig. 6,7; Table 4). According to the preponderance of lime-based binders, CaO consistently shows high concentrations throughout all examined samples, reaching or even surpassing 90 weight percent in many instances. Simultaneously, SiO_2 values often fall between 10 and 15 wt.%, indicating the mortar matrix's contribution from siliceous aggregates and/or secondary reaction products.

Table 4 summarizes the classification of the samples based on their MgO content, as determined by SEM–EDS analysis, which emerges as a key discriminant parameter. A subset of the mortars contains calcitic binders enriched in magnesium, suggesting the use of dolomitic or partially dolomitized limestone sources. Interestingly, as seen in Fig. 7, mortars from the lower level of the Bailelekas tower contain detectable levels of magnesium, but those from the upper level do not. The North Mytikas tower shows a similar stratigraphic differential, with mortars from the lower construction period showing significantly higher magnesium contents than those from the upper level.

Overall, these observations provide preliminary compositional evidence for variability between different construction phases. A total of five mortar samples from different building levels of the Bailelekas tower and four samples from the North Mytikas tower were examined, allowing for a preliminary evaluation of the technological decisions and raw material selections made throughout the various phases of construction (Fig. 8).

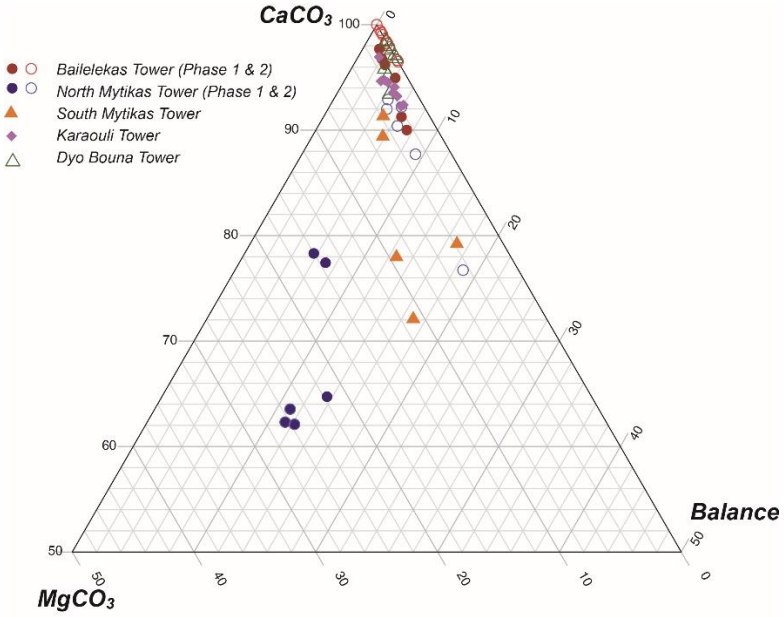


Fig. 7 Ternary diagram of $CaCO_3$, $MgCO_3$ and the balance, which corresponds to the sum of the remaining compounds, determined by SEM-EDS: The symbols indicate the individual towers from which the mortar samples were collected.

Table 4 Chemical characterization of mortars from the examined towers by SEM–EDS and pXRF, and statistical classification of samples based on MgO content (nd=below detection limit).

Classified as Internal | Intern

SAMPLES	CaO	SiO2	MgO	Al2O3	Na2O	MnO	K2O	Fe2O3
B1	96.12	3.46	nd	nd	nd	nd	nd	nd
B2	99.19	nd	nd	nd	nd	1.35	nd	nd
B3	95.80	4.20	nd	nd	nd	nd	nd	nd
B4	95.56	2.84	0.94	0.66	nd	nd	nd	nd
B5	88.23	4.97	1.59	nd	2.39	2.82	nd	nd
NM4	70.63	12.29	14.47	1.24	nd	nd	1.36	nd
NM2	59.52	16.20	20.91	1.10	nd	1.32	2.57	nd
NM3	89.15	7.06	2.11	1.68	nd	nd	nd	nd
NM1	78.57	11.48	2.77	1.39	nd	4.14	1.64	nd
SM1	81.59	13.33	3.32	1.57	0.97	nd	0.58	nd
SM2	68.19	12.16	7.88	nd	10.10	nd	1.67	nd
K1	93.73	3.61	1.58	1.08	nd	nd	nd	nd
K2	90.56	6.60	1.43	1.41	nd	nd	nd	nd
K3	89.62	6.50	1.42	1.32	nd	nd	nd	1.14
DV1	95.04	3.90		1.07	nd	nd	nd	nd
DV2	93.97	3.79	1.55	1.24	nd	nd	nd	1.15
DV3	95.52	3.69	1.27	1.11	nd	nd	nd	nd

Towers of Euboea: MgO content			
Bailelekas	1B, 2B, 3B	LDL	Upper part
	4B, 5B	1-1.6%	Lower part
North Mytikas	1NM, 3NM	2-2.8%	Upper part
	2NM, 4NM	15-21%	Lower part
South Mytikas	1SM, 2SM	3.3-7.9%	----------
Dyo Vouna	1DV, 2DV, 3DV	1-1.2%	----------
Karaouli	1K, 2K, 3K	1.4-1.6%	----------

Classified as Internal | Intern

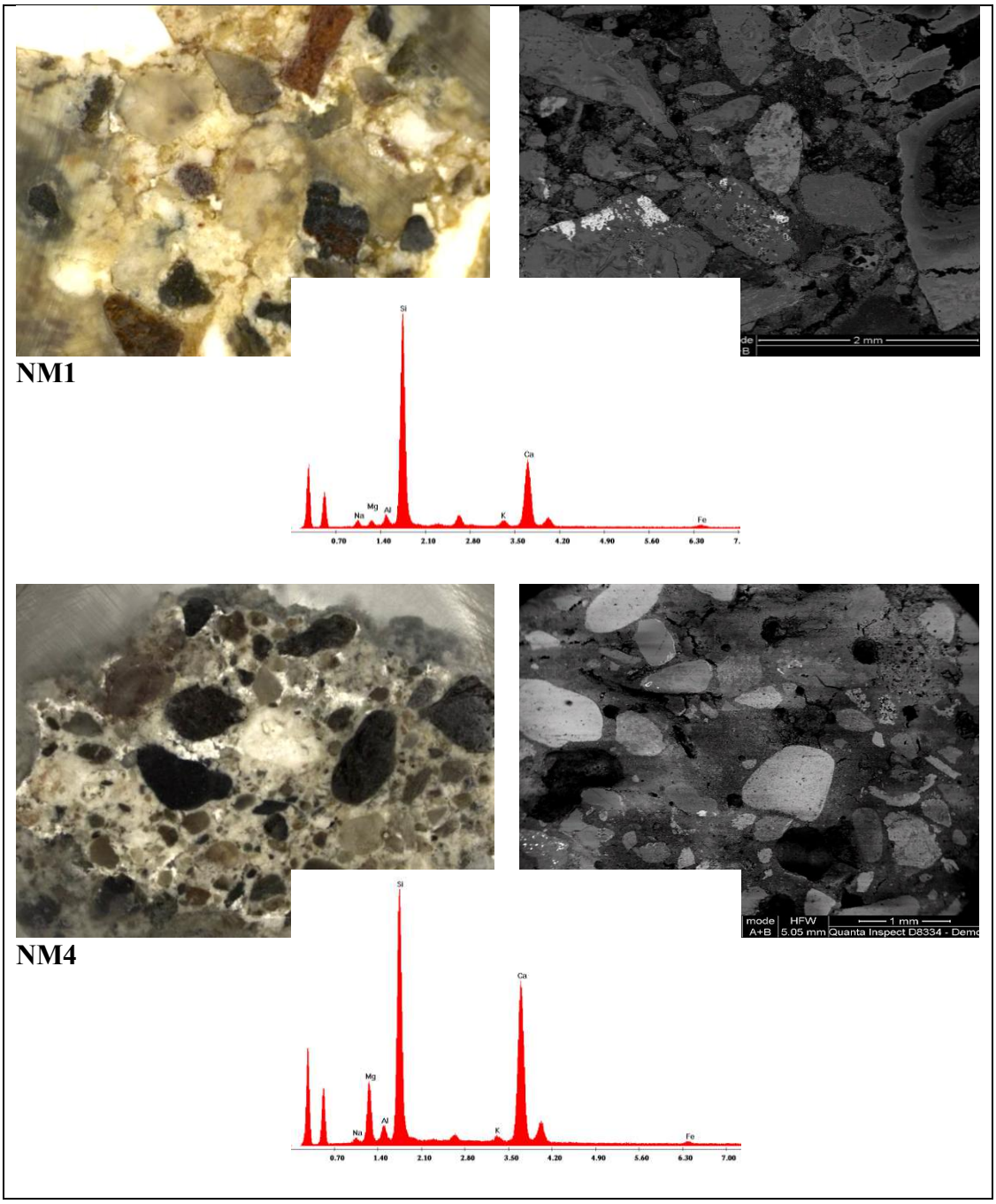


Fig. 8 Representative optical microscopy (OM) and SEM–EDS images illustrating the upper (NM1) and lower (NM4) part of the North Mytikas Tower and the presence of Mg in the lower part.

3.4 Thin sections and mineralogy

Thin-section petrographic analysis of six representative mortar samples enabled a preliminary classification based on their geological constituents and technological features related to raw material selection and manufacturing processes. This study made it possible to classify the mortars into different fabric types by revealing observable differences in

Classified as Internal | Intern

aggregate composition, binder properties, and textural correlations. The diagnostic mineralogical and microstructural characteristics of representative polarized-light photomicrographs are presented below (Fig. 9).

The binder of the *sample B2* is texturally homogeneous and exhibits a brownish-beige colour in both PPL and XPL. It is predominantly composed of micritic calcite. Lime lumps are occasionally observed; they are discernible mainly under crossed polars and display yellowish to light-grey interference colours. The binder-to-aggregate ratio ranges between approximately 55/45 and 60/40. Aggregates are poorly sorted, with a maximum grain size of up to 5.4 mm. They are dominated by subrounded to subangular micritic limestone fragments, while subangular serpentinite clasts are abundant. Microsparitic to sparitic limestone, as well as bioclastic limestone fragments, occur in common to minor amounts. Sandstone, siltstone, and shale fragments are present in comparable proportions, whereas schist fragments and quartzite occur only sporadically. Several sedimentary, metamorphic, and serpentinite clasts locally display thin rims of microcrystalline calcite, indicating partial interaction with the carbonate binder. Rare metamorphic fragments composed of quartz and garnet are also identified. Chert occurs in trace amounts. Sporadic orange–reddish fragments are tentatively interpreted as ceramic (pottery) inclusions.

Sample B5 is compositionally comparable to sample B2 but displays distinct textural features. The binder is brownish-beige and consists mainly of micritic calcite, locally associated with cryptocrystalline calcite. Lime lumps are very common and, in some cases, reach considerable dimensions (up to ~5.7 mm). The binder-to-aggregate ratio is approximately 40/60. Aggregates are medium sorted overall, although locally well-sorted microdomains are observed. The maximum grain size reaches ~5 mm, but only for a limited number of clasts. Aggregate composition closely mirrors that of B2, with predominant subrounded to subangular micritic limestone and abundant subangular serpentinite fragments. Microsparitic–sparitic and bioclastic limestone fragments are common to minor. Sandstone, siltstone, and shale fragments occur in similar proportions, while schist and quartzite are occasional. Some sedimentary, metamorphic, and serpentinite clasts exhibit microcrystalline calcite rims. Rare metamorphic fragments composed of clinopyroxene and mica are observed. Chert is rare, and gypsum occurs only in trace amounts. Occasional orange–reddish fragments are again interpreted as possible ceramic inclusions.

Sample K3 is petrographically similar to samples B2 and B5; however, it is distinguished by a higher degree of aggregate rounding and a clearly biogenic character of the limestone fraction. The limestone aggregates contain abundant microfossils, and isolated microfossils are also dispersed within the matrix. Some serpentinite fragments preserve relict olivine. Calcite-rimmed clasts are less frequent than in samples B2 and B5. The binder is homogeneous, brownish-beige in colour, and composed of micritic calcite. Lime lumps were not observed. The binder-to-aggregate ratio is approximately 40/60. Aggregates are medium to well sorted, with a maximum grain size of up to 5.4 mm. Sporadic hematite grains are present.

The binder in *sample DV2* is less homogeneous than that of sample K3 and locally exhibits a patchy appearance. It is brownish-beige and composed of micritic calcite. Lime lumps are occasionally present. The binder-to-aggregate ratio is approximately 40/60. Aggregates are poorly to moderately sorted and reach a maximum grain size of up to 6.5 mm. The aggregate assemblage is compositionally very similar to that of sample K3, including biogenic limestone and serpentinite fragments, and likewise contains sporadic hematite grains.

The binder in *sample NM4* is distinctly darker brown than in the other examined samples and is texturally inhomogeneous. It is mainly composed of micritic calcite, with subordinate cryptocrystalline calcite. Lime lumps are difficult to identify. This sample exhibits the coarsest aggregate population among all examined mortars, with maximum grain sizes reaching up to ~7 mm. The binder-to-aggregate ratio is very low, approximately 15/85 to 20/80, and the aggregates are very poorly sorted. Metamorphic lithic fragments predominate, consisting mainly of quartzite and abundant muscovite schist and slate. Many of these fragments appear to derive from deformed, metamorphosed granitic protoliths. Subrounded sparitic to microsparitic calcite fragments are very rare. Serpentinite clasts are only sporadically encountered.

Sample SM3 is characterized by a markedly inhomogeneous binder containing a significant amount of porosity, mainly in the form of randomly distributed channel-like voids, accounting for approximately 15% of the binder volume. The binder is strongly amalgamated with calcareous components and displays a brown colour. It consists of micritic and cryptocrystalline calcite. Lime lumps are very common and exhibit dark grey to dark brown colours. The binder-to-

Classified as Internal | Intern

aggregate ratio is high, approximately 75/25. Aggregates are poorly sorted, with a maximum grain size of up to 9.5 mm. Serpentinite fragments are completely absent. Metamorphic lithic fragments dominate and consist mainly of quartzite, with minor muscovite schist and rare chlorite schist. Calcareous fragments are difficult to distinguish due to their partial assimilation into the binder. Chert occurs in rare to very minor amounts.

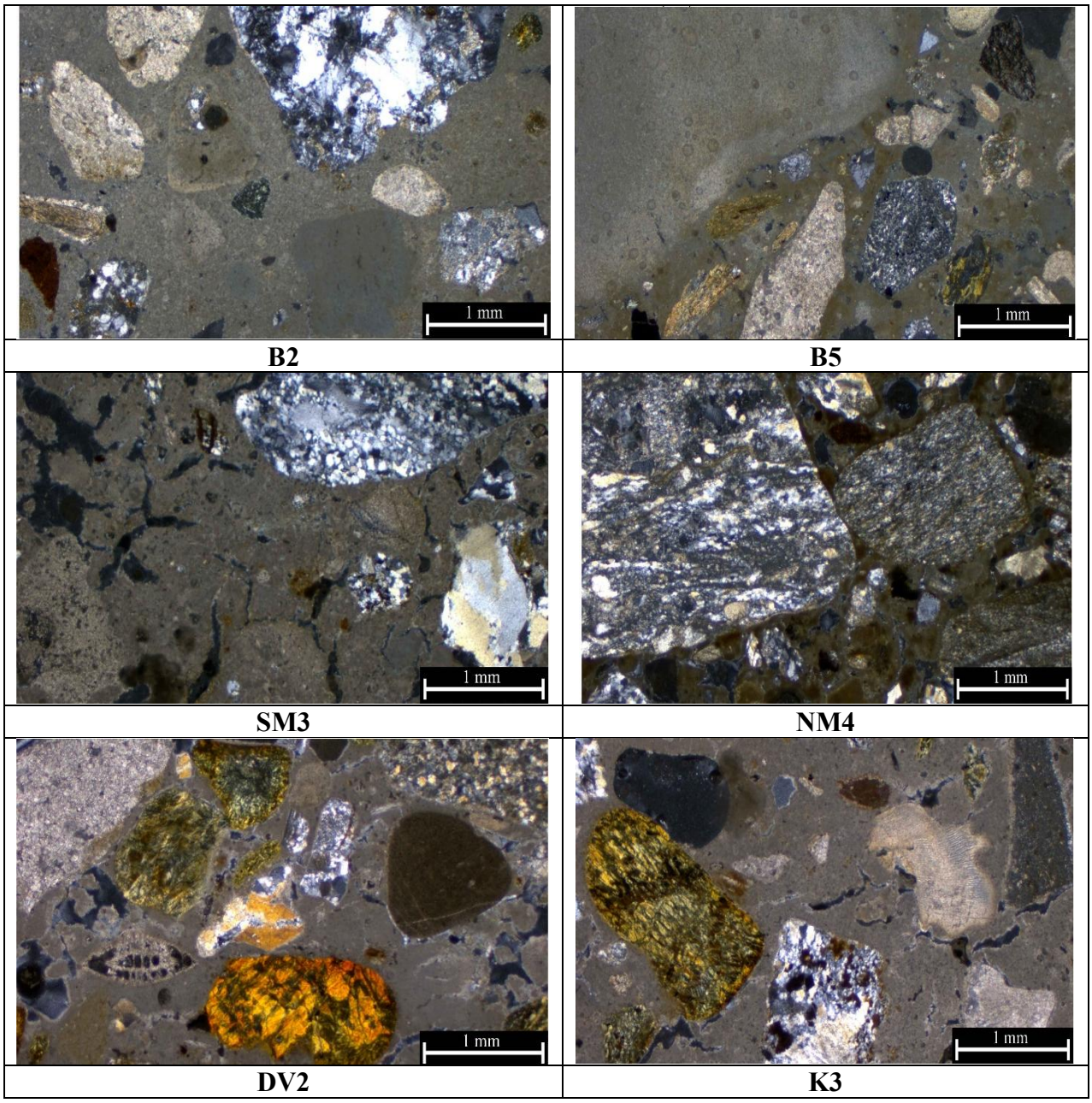


Fig. 9 Representative photomicrographs of fabric mortars identified in the study, crossed polars (XP).

Classified as Internal | Intern

3.5 X-Ray Diffraction analysis

The examined samples exhibit a mineralogical composition that is strongly controlled by the geological background of each sampling location, as clearly demonstrated by their X-ray diffraction (XRD) patterns (Table 5). In contrast, no substantial intra-compositional variability was detected among samples collected from the same tower, indicating a relatively homogeneous selection of raw materials within each construction unit.

Calcite and quartz are ubiquitous constituents in all samples, with calcite prevailing in the majority of cases. An opposite trend, characterized by quartz contents exceeding those of calcite, is observed in most samples from the North and South Mytikas Towers, whereas the two phases occur in broadly comparable proportions in the Dyo Vouna.

Illite/muscovite and plagioclase are also present in most samples, albeit in subordinate amounts. Notable exceptions include samples B5 and BM1 from the Bailelekas and North Mytikas Towers, respectively, in which muscovite is absent, as well as the samples from the Dyo Vouna Tower, where plagioclase was not detected.

In towers located in proximity to ophiolitic lithologies, namely Bailelekas, Dyo Vouna, and Karaouli, serpentine-group minerals (lizardite/antigorite) are systematically identified. In some cases, these phases are accompanied by traces of clinopyroxene, particularly in samples from the Bailelekas Tower, reflecting the local ultramafic geological substratum.

Clay minerals of the montmorillonite–chlorite group occur less frequently but may contribute in appreciable amounts, being identified in approximately half of the samples from the Bailelekas and North Mytikas Towers. Mixed-layer clay minerals were detected only in a single Bailelekas sample.

Secondary and accessory mineral phases include gypsum, which is present in most samples from the North Mytikas Tower and in one sample from the South Mytikas Tower, as well as hematite, detected in minor quantities in some North Mytikas samples and consistently in all samples from the DyoVouna Tower. Vesuvianite was identified exclusively in two samples from the North Mytikas Tower, while olivine was observed only in sample B3 from Bailelekas. Finally, K-feldspar was detected solely in sample NM3 from the South Mytikas Tower.

Classified as Internal | Intern

Table 5 X-Ray Diffraction analysis of the examined mortar samples.

Sample ID	Petro-fabric	Quartz	Calcite	Illite/ Muscovite	Montmori-llonite - Chlorite	mixed layer clays	Plagioclase	K-Feldspar	Pyroxene	Antigorite/ Lizardite	Olivine ?	Gypsum	Vesuvianite	Hematite
B1		++	+++	tr/+	+/++	-	tr	-	tr/+	+	-	-	-	-
B2	fabric 2	++	+++	+	-	+/++	tr	-	tr/+	+	-	-	-	-
B3		++	+++	+	-	-	tr	-	-	+	+	-	-	-
B4		++	+++	+	+/++	-	tr/+	-	-	+	-	-	-	-
B5	fabric 2	++	+++	-	-	-	tr	-	tr/+	+	-	-	-	-
BM1		+++	++	-	-	-	tr/+	-	-	-	-	+	tr/+	tr/+
BM2		+++	++	tr	-	-	+	-	-	-	-	+	+	+
BM3		++	+++	tr/+	+/++	-	+	-	-	-	-	-	-	-
BM4-SLR2294	fabric 4	+++	+	+	tr/+	-	+	-	-	-	-	tr	-	-
DB1		+++	+++	tr/+	-	-	-	-	-	+	-	-	-	tr/+
DB2	fabric 1	+++	+++	tr/+	-	-	-	-	-	+	-	-	-	tr/+
DB3		+++	+++	tr/+	-	-	-	-	-	+	-	-	-	tr/+
K2-SLR2294		++	+++	tr	-	-	tr/+	-	-	+	-	-	-	-
K3-SLR2294	fabric 1	++	+++	tr	-	-	tr/+	-	-	+	-	-	-	-
NM1-SLR2294		++	+++	tr	-	-	tr/+	-	-	-	-	-	-	-
NM2-SLR2294		+++	+++	tr	-	-	tr/+	-	-	-	-	+	-	-
NM3-SLR2294	fabric 3	+++	++	tr/+	-	-	+/++	+	-	-	-	-	-	-

-: not detected; tr: traces; +: few; ++: common; +++: frequent; ++++: abundant; +++++: dominant

Classified as Internal | Intern

4. DISCUSSION AND INTERPRETATION OF THE RESULTS

4.1 Radiocarbon dating

The radiocarbon results indicate that all six towers and their dated phases were constructed within the period 1270–1434 cal AD. For two beams from Skounteri and North Mytikas, Wiggle Matching analysis provided more precise construction dates. Specifically, Skounteri-2 (lower phase) dates to 1396–1418 cal AD, while North Mytikas-2 (upper phase) dates to 1334–1374 cal AD, indicating that the upper phase of North Mytikas predates that of Skounteri.

Figure 10 presents the calibrated radiocarbon age ranges, corrected for missing rings, for all towers (Table 2), arranged from oldest to youngest. Where two samples derived from the same construction phase, as suggested by masonry characteristics (Mistros, South Mytikas, and Bailelekas), the dates were statistically combined. For Skounteri and North Mytikas, Wiggle Matching was applied to samples Skounteri-2 and North Mytikas-2 (Figure 2), yielding high-precision dates (Table 4), which were subsequently combined with dates from Skounteri-1 and North Mytikas-1, respectively, as these likely belong to the same construction phase.

Figure 10 shows that the combined date of the two Mistros tower samples (DEM-2974 and DEM-2973) yields the earliest age (ca. 1300 cal AD), located on a smooth section of the calibration curve and therefore more precise than the others. In contrast, North Mytikas and Skounteri are clearly younger, with Skounteri the most recent (ca. 1400 cal AD). The dates for Karaouli, Bailelekas, and South Mytikas fall within a wiggle in the calibration curve, producing two sub-ranges within the 95.4% probability interval (Section 4.3; Figure 8). This results in two possible chronological placements: either contemporaneous with Mistros or with Skounteri. Karaouli and Bailelekas show probabilities of 52.9% and 68.2%, respectively, of aligning with Mistros (1280–1330 AD), while South Mytikas has a 70.1% probability of falling between the two groups. However, the probabilities of the younger ranges (42.5%, 27.3%, and 25.4%, respectively) remain significant, allowing for synchrony with Skounteri. A more refined chronological ordering of the towers could consider their construction phases; however, such phases are generally difficult to distinguish. In most cases, the sampled wood derives from a single, likely primary, construction phase. Exceptions may be identified at Bailelekas and North Mytikas, where two phases can be tentatively recognized (Figure 2). In both cases, the sampled wood originates from the upper phase, where timber elements are preserved.Accordingly, the initial construction of these towers likely predates the obtained radiocarbon dates. For Bailelekas, the upper phase dates to 1270–1310 cal AD (68.2%) or alternatively 1364–1384 cal AD (27.3%), indicating that the lower phase—and thus the initial construction—must be earlier, reinforcing the likelihood of the older range. Similarly, the lower phase of North Mytikas must predate the upper phase dated to 1334–1374 cal AD.

Classified as Internal | Intern

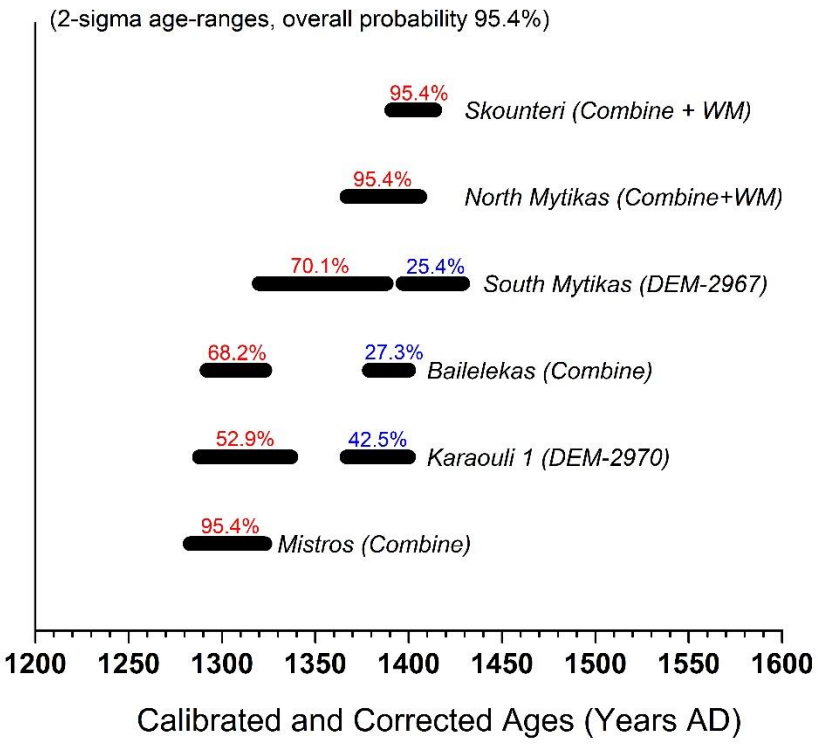


Fig. 10 Calibrated radiocarbon ages ranges corrected for mission rings for all Towers studied according to Table 3. See text for details.

Classified as Internal | Intern

4.2 Mortar Analysis

In the present study, the Bailelekas and North Mytikas towers were sampled at two distinct stratigraphic levels corresponding to their lower and upper structural parts. This approach was based on preliminary analyses aimed at identifying potential differences between earlier and later construction phases. In both towers, mortar samples from different heights display clear compositional variation, providing strong evidence for two distinct technological phases (Fig. 7). This interpretation is supported by optical microscopy and petrographic analysis, as well as by systematic differences in elemental ratios (e.g., Ca/Si, Sr/Si, Fe/Si) obtained through SEM–EDS. XRD and geochemical data further indicate compositional affinities among groups of towers.

Mortars from Bailelekas, Karaouli, and Dyo Vouna exhibit broadly similar chemical characteristics, whereas those from North and South Mytikas form a distinct compositional group (Fig. 6). Some samples, particularly from South Mytikas, show significant deterioration, which may affect their analytical signatures. Despite these differences, all towers fall within a broadly similar chronological framework. Notably, Bailelekas and North Mytikas preserve evidence of two technologically distinct mortar phases, indicating episodes of modification or rebuilding. However, only six thin sections were suitable for petrographic analysis due to extensive sample deterioration, limiting detailed comparison, particularly for the upper phase of North Mytikas, which could not be assessed to the same extent as Bailelekas.

With regard to the petrographic results, only preliminary conclusions can be drawn due to the limited number of analysed thin sections (six in total). Nevertheless, a consistent technological pattern is evident: alongside calcite, locally available lithologies were systematically used as aggregate material. The frequent occurrence of metamorphic rock fragments in North and South Mytikas is consistent with their proximity to lacustrine and fluvial–terrestrial deposits in the Eretria area, rich in sandstones and sandy marls. Fabrics 1 and 2 are further distinguished by the presence of serpentine and calcareous components. The predominance of serpentine in Karaouli and Dyo Vouna, and to a lesser extent in Bailelekas, aligns with their location within the influence zone of the ophiolitic complex near Psachna, dated to the Upper Jurassic–Lower Cretaceous.

The presence of lime lumps in Fabrics 1, 2, and 3 is also noteworthy, as such features in historical mortars are commonly associated with incomplete calcination (Leslie and Hughes 2002; Philokyprou 2012). Their identification in five of the analysed samples suggests a shared practice in lime production, with the exception of South Mytikas, where such inclusions were not observed. Notably, Fabric 1 occurs in both Karaouli and Dyo Vouna, indicating the use of similar raw materials and preparation techniques. Moreover, this technological continuity appears to persist over time, as evidenced at Bailelekas, where no petrographic differences were identified between mortars from the lower and upper construction phases.

Classified as Internal | Intern

5. CONCLUSIONS AND HISTORICAL CONTEXT

Within the framework of the present pilot study an integrated methodological approach has been developed for investigating the medieval towers of Euboea through the combined application of radiocarbon dating of wooden beams and the compositional and microstructural characterization of mortars. The approach is particularly adapted in view of the exposed mountainous locations of the towers and the microclimate of the island of Euboea. The correlated environmental conditions have accelerated material deterioration, which in some cases even resulted in the complete loss of wooden beams. By integrating scientific analyses, the methodology enables the reconstruction of building phases and construction practices despite challenging preservation and accessibility conditions. Based on the work flow and the collected results of the present pilot study the approach can be advanced for broader comparative research.

Construction wood beams from six towers were radiocarbon dated using the outermost preserved tree rings. Missing rings beneath the bark were estimated based on curvature and ring-width patterns, allowing closer approximation to the tree-felling date and, by extension, the construction date. Results indicate that the towers were built within the broad range of 1270–1434 calAD. A calibration-curve wiggle within this interval produced two possible sub-ranges (c. 1280/1320–1370/1390 calAD and c. 1370/1390–1410/1430 calAD) for some samples. However, Wiggle Matching and the combination of samples from the same construction phase yielded refined dates for three towers: Mistros (1283–1323 calAD; mean 1303 ± 19), North Mytikas (1330–1374 calAD; mean 1352 ± 22), and Skounteri (1391–1414 calAD; mean 1402 ± 11). These results establish a construction sequence with Mistros as the earliest and Skounteri as the latest. For the remaining towers (Bailelekas, South Mytikas, and Karaouli), the calibration split could not be resolved; nevertheless, their construction likely falls between the dates established for Mistros and Skounteri.

Although radiocarbon (^{14}C) dating constitutes the primary chronological tool, the absence of wooden elements in the lower sections of the Bailelekas and North Mytikas towers precluded the independent dating of their respective construction phases. Consequently, mortar analysis emerged as a critical alternative approach, despite the inherent limitations imposed by the restricted number of available samples. At both towers, distinct upper and lower construction phases were identified, with the lower parts representing the earlier phase. In Bailelekas, clear differences in mortar technology between these phases suggest a chronological gap, which, in combination with the radiocarbon data, supports an initial construction date around 1364–1384 cal AD or earlier. These distinctions are based on variations in chemical and petrographic characteristics identified through pXRF, SEM–EDS, and thin-section analysis, within the framework of a pilot study aimed at developing an integrated methodological approach. Despite the small number of thin sections analysed (n = 6), petrographic evidence further supports technological variability. While some samples (e.g., B2 and B5) exhibit similar raw materials, they differ significantly in microstructural features such as binder homogeneity, lime lump characteristics, binder-to-aggregate ratios, and aggregate sorting. These differences indicate variations in mortar preparation and application techniques, suggesting that similar materials were employed through distinct technological processes, likely reflecting differences in construction phases, workmanship, or functional requirements.

This time alignment implies that the towers were the result of several construction and reinforcing periods in response to shifting military and administrative requirements rather than a single, cohesive defensive strategy. The dated construction phases, which cover the late 13th to the early 15th century, largely correspond with the region's consecutive periods of Lombard and Venetian control of the island of Euboea, and Catalan and Florentine annexation of the mainland. This time alignment implies that the towers were the result of several construction and reinforcing periods in response to shifting military and administrative requirements rather than a single, cohesive defensive strategy. It is possible to hypothesize that the Mistros (1283-1323 calAD) tower, which preserves one observation slit, indicating its use for signal recognition, was constructed in the early fourteenth century in a strategic mountain position (perhaps as part of a wider island communication network) in response to the threat of Turkish and

Classified as Internal | Intern

Catalan corsairs. As the security situation deteriorated further in the 1330's under increasing Turkish threats, landlords began to fortify their estate centres to provide secure storage of agricultural production and ensure the safety of themselves and their villagers (e.g. North Mytikas tower (1330-1374 CE.): this is similar to tower-construction by monastic institutions of Byzantine-controlled northern Greece in the same period. In 1390 the Venetians incorporated Euboea into their empire: the construction of the Skounteri tower (1391-1414) can be seen as part of a co-ordinated strategy, as on other islands under their control, to create a potential chain of signal and observation towers linking the north and south of the island and perhaps its other island possessions in the Aegean (Blackler, 2022).

This interpretation is further supported by the petrographic and geochemical analyses of the mortars, which reveal distinct preparation strategies and the selective use of local raw materials. The identification of discrete construction phases inside certain towers, like North Mytikas and Bailelekas, highlights the complexity of their architectural history. Although the absence of wooden elements prevents the independent chronological attribution of these phases, their material differentiation strongly suggests episodes of repair or rebuilding. Overall, the combined use of historical evidence, high-resolution radiocarbon dating, and mineralogical characterization demonstrates the considerable potential of an integrated approach for reconstructing the chronology, technology, and function of medieval defensive structures in the region.

Acknowledgements

The authors express their sincere gratitude to the Ephorate of Antiquities of Euboea for granting permission to conduct this research and for their support during fieldwork. They particularly thank the Director, Dr. Dimitrios Christodoulou, and his predecessors for their valuable collaboration. Financial support from the UK-based Castle Studies Trust is gratefully acknowledged. The authors also thank Mrs Marigo Eirini Kyriazi of the Radiocarbon Unit at NCSR "Demokritos" for her assistance with the preparation and pretreatment of the wood samples.

Classified as Internal | Intern

Author Declarations

Funding

Author D, Andrew Blackler, has received research funding from the UK-based Castle Studies.

Conflicts of Interest / Competing Interests

The authors declare that there are no conflicts of interest or competing interests related to this study. All financial, personal, or professional relationships that could be perceived to influence the work reported in this manuscript have been disclosed. Any funding sources or affiliations that might be viewed as potential conflicts have been transparently acknowledged in the relevant sections of the manuscript.

Ethics approval/declarations

All necessary permissions for sampling and analysis of archaeological materials were obtained from the relevant authorities. The study complies with national and international guidelines for the treatment of cultural heritage materials. No living human participants or animals were involved, and all destructive analyses were carried out under approved protocols to minimize damage to the specimens.

Consent to Participate

This study did not involve living human participants. All archaeological materials analyzed were obtained with the necessary permissions from the respective authorities. Consent for sampling and analysis was granted by these authorities in accordance with relevant legal and ethical guidelines.

Consent for Publication

Not applicable. The study does not include identifiable human data. All permissions to publish results derived from the analyzed archaeological materials were obtained from the relevant authorities.

Availability of data and material/ Data availability

The datasets generated and/or analyzed during the current study are available from the corresponding author on reasonable request. Any supplementary material, including raw measurement data, images, or sample metadata, has been deposited in NCSR Demokritos.

Code Availability

Any custom code, scripts, or software used for data analysis in this study are available from the corresponding author upon reasonable request.

Classified as Internal | Intern

BIBLIOGRAPHY

Ali A, Chiang YW, and Santos RM (2022) X-ray diffraction techniques for mineral characterization: A review for engineers of the fundamentals, applications, and research directions. *Minerals*, 12(2), 205. doi: 10.3390/min12020205

Aškrabić A, Zakić M, Savić D, Miličić A, Delić-Nikolić L, and Vyšvařil I (2023) Determination of the salt distribution in the lime-based mortar samples using XRF and SEM-EDX characterization. In V. Bokan Bosiljkov, A. Padovnik, & T. Turk (Eds.), *Conservation and Restoration of Historic Mortars and Masonry Structures*. HMC 2022. RILEM Bookseries (Vol. 42). Springer, Cham. doi: 10.1007/978-3-031-31472-8_43

Bezur L, Lee M, Loubser M, and Trentelman K (2019) *Hand-held XRF in cultural heritage: A practical workbook for conservators*. Getty Conservation Institute.

Blackler A (2020) The Medieval Landscape of Euboea (Negroponte): A Framework for Interpreting the Byzantine and Frankish Towers of Greece, *Unpublished Doctoral Thesis*, University of Birmingham, UK.

Blackler A (2022) Communication and the Role of the Medieval Tower in Greece: a Re-appraisal. *Annual of the British School at Athens*, 117, 393-414.

Bronk Ramsey C (2021) Oxcal v4.4.4 calibration program, https://c14.arch.ox.ac.uk/oxcal.html.

Bronk Ramsey C, van der Plicht H, and Weninger BP (2001) 'Wiggle matching' radiocarbon dates, *Radiocarbon* 43(2A), 381–389. doi:10.1017/S0033822200038248

Bullock P (1985) *Handbook for Soil Thin Section Description*, Wolverhampton: Waine Research.

Cantisani E, Fratini F, and Pecchioni E (2022) Optical and electronic microscope for minero-petrographic and microchemical studies of lime binders of ancient mortars. *Minerals*, 12(1), 41. doi: 10.3390/min12010041

Chuo RA, Nyangi P, and Kifanyi G (2024) Chemical, mineralogical, and petrographic analysis of the mud mortar from Fort Ikoma historical building in Serengeti National Park, Tanzania. *Journal of Applied Sciences and Environmental Management*, 28(9), 2767–2775.doi: 10.4314/jasem.v28i9.

Divya Rani S, Rahul AV, and Santhanam M (2021) A multi-analytical approach for pore structure assessment in historic lime mortars. *Construction and Building Materials*, 272, 121905.doi: 10.1016/j.conbuildmat.2020.121905

Elsen J (2006) Microscopy of historic mortars - a review. Cement and Concrete Research, 36, 1416–1424. https://doi.org/10.1016/j.cemconres.2005.12.006

Ergenç D, Fort R, Varas-Muriel MJ, and Alvarez de Buergo M (2021) Mortars and plasters-How to characterize aerial mortars and plasters. *Archaeological and Anthropological Sciences*, 13, 197. doi: 10.1007/s12520-021-01398-x

Fort R, Varas-Muriel MJ, Ergenç D, Cassar J, Anastasi M, and Vella NC (2023) The technology of ancient lime mortars from the Żejtun Roman Villa (Malta). *Archaeological and Anthropological Sciences*, 15, 15.doi: 10.1007/s12520-022-01710-3

Fort R, Varas-Muriel MJ, Zoghlami K, Ergenç D, and Zaddem A (2024) Analytical characterisation of 1st- and 2nd-century Roman mortars at the Utica archaeological site (Tunisia): Construction phases and provenance of the raw materials. *Journal of Archaeological Science: Reports*, 54, 104404.doi: 10.1016/j.jasrep.2024.104404

Hein A (2021) Revisiting the groups – Exploring the feasibility of portable EDXRF in provenance studies of transport amphorae in the Eastern Aegean, in: M. Hegewisch, M. Dazkiewicz and G. Schneider (eds.),

Classified as Internal | Intern

Application of Portable Energy-Dispersive X-ray Fluorescence to the Analysis of Archaeological Ceramics and Glass, Vol. 75, Berlin: Topoi -Berlin Studies of the Ancient World, 43-61.doi: 10.17171/3-75

Ghorbani S (2025) The role of petrographic characteristics on the physicomechanical behaviors and drillability of rocks: A comprehensive review. *Discovery Geosciences*, 3, 41.doi: 10.1007/s44288-025-00147-0

Goldstein J, Newbury DE, Joy DC, Lyman CE, Echlin P, Lifshin E, Sawyer L, and Michael JR (2018) *Scanning electron microscopy and X-ray microanalysis*, 4th edition, Springer, Cham. doi: 10.1007/978-1-4939-6676-5

Kostarelli A (2024) 'Ο μεσαιωνικός πύργος στον Ατμοηλεκτρικό Σταθμό Αλιβερίου στην Εύβοια. Παρατηρήσεις μετά τις εργασίες αποκατάστασης', in C. Merantzas, V. Papadopoulou and I. Chouliaras (eds.), *Φῶς Ἱλαρόν: Αφιέρωμα στη Μνήμη του Αθανάσιου Πάλιουρα*, 183-199, Athens: GreekMinistryofCulture.

Kostarelli A, Blackler A forthcoming, The medieval towers of Euboea. New data, perspectives and the restoration works of the Ephorate of Antiquities of Euboea, *Online International Conference on Byzantine, Western and Post-Byzantine Towers (10th-16th centuries)* (Friday 18 - Sunday 20 November 2022),

Kromer B, and Münnich KO (1992) CO2 gas proportional counting in radiocarbon dating- Review and perspective, in: R.E. Taylor, A. Long and R.S. Kra (eds.), *Radiocarbon After Four Decades-An Interdisciplinary Perspective*, New York: Springer-Verlag, 184-197.doi: 10.1007/978-1-4757-4249-7

Langdon MK (1995) The mortared towers of central Greece: an Attic supplement. *The Annual of the British School at Athens*, 90, pp 475-503. doi:10.1017/S0068245400016312

Lancaster LC (2021) Mortars and plasters—How mortars were made: The literary sources, *Archaeological and Anthropological Sciences*, 13, 192. doi: 10.1007/s12520-021-01395-0

Leslie AB, and Hughes JJ (2002) Binder microstructure in lime mortars: Implications for the interpretation of analysis results,*Quarterly Journal of Engineering Geology and Hydrogeology,* 35, 257–263. doi: 10.1144/1470-923601-27

Lock P (1986) The Frankish towers of Central Greece, *The Annual of the British School at Athens* 81**,** 101-123. doi:10.1017/S0068245400020104

Lock P (1989) The medieval towers of Greece: A problem in chronology and function, in: B. Arbel, B. Hamilton and D. Jacoby (eds.), *Special Issue: Latins and Greeks in the Eastern Mediterranean After 1204, Mediterranean Historical Review* 4(1), 129-145.

Lock P (1996) The towers of Euboea: Lombard or Venetian, agrarian or strategic, in: P. Lock and GDR. Sanders (eds.), *The Archaeology of Medieval Greece*, Oxford: Oxbow Monograph 59**,** 107-126.

Loizou C (2017) The medieval towers of Euboea: Their dimension as domestic and landscape phenomena, in: Z. Tankosic, F. Mavridis & M. Kosma (eds.), *An Island Between Two Worlds: The Archaeology of Euboea from Prehistoric to Byzantine Time*s, Papers and Monographs from the Norwegian Institute at Athens 6, Athens: Norwegian Institute at Athens, 625-638.

Maniatis Y, Malamidou D, Koukouli-Chryssanthaki H, and Facorellis Y (2010) Radiocarbon Dating of the Amphipolis Bridge in Northern Greece, Maintained and Functioned for 2500 Years, *Radiocarbon*, **52**(1), 41–63. doi:10.1017/S0033822200045021

Classified as Internal | Intern

Maniatis Y, Oberlin C, and Tsirtsoni Z (2016) 'BALKANS 4000': The Radiocarbon dates from archaeological contexts, in: Z. Tsirtsoni (ed.), *The Human Face of Radiocarbon,* TMO 69, Lyon: Maison de l'Orient et de la Méditerranée, 41-65.

Münnich KO (1957) *Messung naturlichen radiokohlenstoffs mit einem CO2 proportional zahlrohr. Einige anwendungen der methode., Inaugural-dissertation zur erlangung der doktorwurde hohen naturwissenschaftlich-mathematischen fakultat*, Heidelberg: Ruprecht-Karl-Universität.

Nicosia C, and Stoops G (2017) *Archaeological Soil and Sediment Micromorphology*, Hoboken, NJ: John Wiley & Sons.

Pecchioni E, Fratini F, and Cantisani E (2025) Atlas of the Ancient Mortars in Thin Section under Optical Microscope,3rd ed.; Nardini: Florence, Italy, p. 78

Philokyprou M (2013) The Earliest Use of Lime and Gypsum Mortars in Cyprus, *RILEM Bookseries,* Cyprus: University of Cyprus, 7,25-35. doi: 10.1007/978-94-007-4635-0_3

Pineda P, Medina-Carrasco S, Iranzo A, Borau L, and García-Jiménez I (2022) Pore structure and interdisciplinary analyses in Roman mortars: Building techniques and durability factors identification, *Construction and Building Materials*, 317, 125821. doi: 10.1016/j.conbuildmat.2021.125821

Quinn P (2013) *Ceramic Petrography. The Interpretation of Archaeological Pottery and Related Artefacts in Thin Section*, Oxford: Archaeopress. doi:10.1002/gea.21493

Schoch H, Bruns M, Münnich KO, and Münnich M (1980) A Multi-Counter System for High Precision Carbon-14 Measurements,*Radiocarbon* 22(2), 442–447.doi: 10.1017/S0033822200009747

Sium AH, Zachary G, Raphael M, and Mwero J (2025) Minero-petrographical, chemical and physical characterisation of the ancient mortars from Fort Jesus Heritage Site, Mombasa, Kenya, *Case Studies in Construction Materials*, 22, e04483. doi: 10.1016/j.cscm.2025.e04483

Skouras TI (1975) ΟχυρώσειςστηνΕύβοια [Fortifications on Euboia], *Arxeion Euboikon Meleton*, Athens, 327-452.

Skouras TI (2003) Ακρόπολεις - Κάστρα - Πύργοι της Εύβοιας [Acropoli - castles - Towers of Euboea], Nomarchiaki Avtodioikisi Euboias

Stuiver M, and Polach HA (1977) Discussion Reporting of 14C Data, *Radiocarbon* 19(3), 355–363.doi: 10.1017/S0033822200003672

Vries de H, and Barendsen GW (1953) Radio-carbon dating by a proportional counter filled with carbondioxide, *Physica* 19(1), 987–1003. doi: 10.1016/S0031-8914(53)80110-**2**

Vroom J (2003) *After Antiquity. Ceramics and Society in the Aegean from the 7th to the 20th centuries A.C. A Case Study from Boeotia, Central Greece*, Archaeological Studies Leiden University 10, Leiden.

Vroom J (2014) *Byzantine to Modern Pottery in the Aegean. An Introduction and Field Guide. Second and Revised Edition*, Turnhout: Brepols Publishers (first edition: Utrecht, Parnassus Press, 2005).

Vroom J (2022) Shifting Byzantine networks: New light on Chalcis (Euripos/Negroponte) as a centre of production and trade in Greece, in: E. Fiori and M. Trizio (eds.), *The 24th International Congress of Byzantine Studies, Volume 1: Proceedings of the Plenary Sessions*, Venice: Edizioni Ca'Foscari, 453-487.

Vroom J, and Kane S (2025) The Hinterlands of Medieval Chalcis Project Unearths a Medieval Landscape in Rural Greece, The Hinterlands of Medieval Chalcis Project Unearths a Medieval Landscape in Rural Greece - Leiden Archaeology Blog / Leiden Medievalists Blog (7 February 2025).

Classified as Internal | Intern

Vroom J, Kostarelli A, Blackler A, Kalantzis-Papadopoulos D, and Kolvers R (2024) The Hinterland of Medieval Chalkida: A preliminary overview of the 2021 and 2022 fieldwork seasons, *Pharos* 25 (2021-2023), 179-234. https://doi.org/10.2143/PHA.25.0.3293423

Vroom J, Kostarelli A, Blackler A, Kalantzis-Papadopoulos D, Ouellet J, Politis K, Lamprakis D, Kolvers R, and Schenkius M. forthcoming a, The Hinterland of Medieval Chalkida: A preliminary overview of the 2023 fieldwork season, *Pharos* 26 (2024-2025)

Vroom J, Kostarelli A, Kalantzis-Papadopoulos D, Groat N, Lambers L, Hoosbeek M, Ferri M, Gosker J, Kane S, Karagiannis N, Nanetti A, Caniato G, Politis KD, and Lamprakis D forthcoming b, The Hinterland of Medieval Chalkida: A preliminary overview of the 2024 fieldwork season, *Pharos* 27 (2026)

Vroom J, Kalantzis-Papadopoulos D, Karagiannis N, and Kostarelli A forthcoming c, Watchtowers, storehouses or residences? Mapping and understanding the medieval towers of Bailelekas and Pissonas in central Euboea, in: P. Androudis (ed.), *Byzantine, Western and Post-Byzantine Towers.*

*W*hitbread IK (1995) *Greek Transport Amphorae: A Petrological and Archaeological Study.* Athens: British School of Athens.

Xanthopoulou V, and Iliopoulos I (2023) An Insight into the Suitability of Clayey Raw Materials: The Ceramic Provinces of the Northern Peloponnese and South Epirus, Greece. *Buildings* 2023, 13, 473. https://doi.org/10.3390/buildings13020473

Classified as Internal | Intern